

- 3 REEVE, M.: 'Line plant considerations for the optical network', *Trans. R. Soc. London A*, 1989, **329**, pp. 61-70
- 4 FINEGAN, T., and HICKS, A. M.: 'Prediction for the optical performance of a novel passive branched fibre network'. IEE colloq., London, March 1989
- 5 AINSLIE, B. J., CRAIG, S. P., DAVEY, S. T., and WAKEFIELD, B.: 'The fabrication, assessment and optical properties of high concentration Nd³⁺ and Er³⁺ doped silica-based fibres', *Materials Lett.*, 1988, **6**, pp. 139-143
- 6 AINSLIE, B. J., CRAIG, S. P., and DAVEY, S. T.: 'The absorption and fluorescence spectra of rare-earth ions in silica based monomode fibre', *J. Lightwave Technol.*, 1988, **6**, pp. 287-293
- 7 MORTIMORE, D. B., and WRIGHT, J. V.: 'Low-loss joints between dissimilar fibres by tapering fusion splices', *Electron. Lett.*, 1986, **22**, (6), pp. 318-319

EFFECT OF NONLINEAR GAIN ON INTENSITY NOISE IN SINGLE-MODE SEMICONDUCTOR LASERS

Indexing terms: Semiconductor lasers, Noise

The effect of nonlinear gain on the intensity noise of semiconductor lasers is studied by solving the single-mode rate equation with the Langevin noise term. The analytic expressions for the relative intensity noise and the intensity autocorrelation function are obtained by using a form of the nonlinear gain that is valid even at high operating power levels. These are used to obtain a simple expression for the signal-to-noise ratio (SNR) of the laser output. The SNR is found to saturate to a limiting value of about 30 dB at high powers because of the nonlinear-gain effects related to intraband gain saturation.

The output of semiconductor lasers exhibits both intensity and phase fluctuations whose origins are related to spontaneous emission that always accompanies stimulated emission.¹ Phase noise manifests itself through the laser linewidth.² Considerable attention has focused on linewidth saturation and the physical mechanism behind it.³⁻⁸ It was shown recently that the nonlinear gain can lead to linewidth saturation.⁸ The nonlinear gain is also expected to affect the intensity noise considerably. However, its effect on intensity noise has attracted little attention.⁹ This Letter studies how intensity noise in semiconductor lasers is affected by intraband gain saturation, a phenomenon responsible for the nonlinear gain. The results show that the signal-to-noise ratio of the laser intensity saturates to a limiting value of about 30 dB because of the nonlinear-gain effects in semiconductor lasers.

The intensity noise for single-mode lasers can be studied by solving the rate equations¹

$$\dot{P} = (G - \tau_p^{-1})P + R_{sp} + F_P(t) \quad (1)$$

$$\dot{N} = I/q - N/\tau_e - GP + F_N(t) \quad (2)$$

where P and N represent the number of photons and electrons inside the active region, τ_p is the photon lifetime, τ_e is the carrier lifetime, R_{sp} is the rate of spontaneous emission into the lasing mode, I is the injection current, and G is related to the gain g by the relation $G = \Gamma v_g g$, where Γ is the confinement factor and v_g is the group velocity. The Langevin noise sources $F_P(t)$ and $F_N(t)$ represent Gaussian stochastic processes of zero mean. They are delta correlated (white noise) in the Markoffian approximation, i.e. $\langle F_i(t)F_j(t') \rangle = 2D_{ij}\delta(t-t')$, where D_{ij} is the diffusion constant with $i, j = P$ or N . Explicitly $D_{PP} = R_{sp}P$, $D_{NN} = R_{sp}P + N/\tau_e$, and $D_{PN} = -R_{sp}P$.

Intraband gain saturation reduces the optical gain at high power levels. By using the density-matrix formalism for a single-mode semiconductor laser, G in eqns. 1 and 2 is given by⁹

$$G(N, P) = G_N(N - N_0)(1 + P/P_s)^{-1/2} \quad (3)$$

where G_N is the differential gain, N_0 is the transparency value

of N , and the saturation photon number P_s is related to the intraband relaxation times as⁹

$$P_s = \frac{\epsilon_0 \hbar n_g V}{\mu^2 \omega_0 \Gamma \tau_{in} (\tau_c + \tau_e)} \quad (4)$$

where \bar{n} is the mode index, n_g is the group index, V is the active volume, μ is the dipole moment, ω_0 is the optical frequency, τ_{in} is the dipole relaxation time, and τ_c and τ_e are the intraband population relaxation times. Typical values of P_s for index-guided InGaAsP lasers are in the range $2-6 \times 10^6$ and correspond to an output saturation power in the range 20-100 mW depending on what fraction of intracavity photons escapes from the output facet.

Intensity noise can be studied by calculating the normalised autocorrelation function $C(\tau)$ defined as

$$C(\tau) = \langle \delta P(t) \delta P(t + \tau) \rangle / \bar{P}^2 \quad (5)$$

where $\delta P = P - \bar{P}$ is the intensity fluctuation from the average value \bar{P} . The Fourier transform of $C(\tau)$ provides the relative-intensity-noise (RIN) spectrum according to the relation

$$C(\tau) = \frac{1}{2\pi} \int_{-\infty}^{\infty} RIN(\omega) \exp(i\omega\tau) d\omega \quad (6)$$

For a semiconductor laser biased above threshold the RIN can be calculated¹ by assuming $\delta P/\bar{P} \ll 1$ and linearising the rate equations in δP and δN , where $\delta N = N - \bar{N}$ is the carrier fluctuation. The result is⁹

$$RIN(\omega) = \frac{2R_{sp}[(\Gamma_N^2 + \omega^2) + G_N^2 P^2(1+p)^{-1}(1+N/R_{sp}P\tau_e)]}{P[(\Omega_R^2 - \omega^2)^2 + (2\omega\Gamma_R)^2]} \quad (7)$$

where the frequency Ω_R and the damping rate Γ_R of relaxation oscillations are given by

$$\Omega_R = \left[\frac{G_N P}{\tau_p} \frac{1+p/2}{(1+p)^2} - \frac{1}{4}(\Gamma_p - \Gamma_N)^2 \right]^{1/2} \\ \Gamma_R = \frac{1}{2}(\Gamma_N + \Gamma_p) \quad (8)$$

and

$$\Gamma_N = \tau_e^{-1} + N \frac{\partial \tau_e^{-1}}{\partial N} + \frac{G_N P}{(1+p)^{1/2}} \quad (9)$$

$$\Gamma_p = R_{sp}/P + p/[2\tau_p(1+p)^{3/2}] \quad (10)$$

The bar over P and N has been omitted in eqns. 7-10 for notational simplicity. The dimensionless parameter $p = P/P_s$ is a measure of nonlinear gain. For $p \ll 1$ eqn. 7 reduces to the well known expression of RIN.¹ At a given frequency and output power the RIN is found to increase for larger values of p indicating that the nonlinear gain enhances the RIN.

The intensity autocorrelation function is obtained by using eqns. 6 and 7 and performing the integration through the method of contour integration. The result is

$$C(\tau) = \frac{R_{sp} \exp(-\Gamma_R \tau)}{2\Gamma_R P} \\ \times \text{Re} \left[\frac{\Gamma_e^2 + (\Omega_R + i\Gamma_R)^2}{\Omega_R(\Omega_R + i\Gamma_R)} \exp(i\Omega_R \tau) \right] \quad (11)$$

where

$$\Gamma_e^2 = \Gamma_N^2 + G_N^2 P^2(1+p)^{-1}[1 + N/(R_{sp}\tau_e P)] \quad (12)$$

Fig. 1 shows temporal variation of $C(\tau)$ for several output powers by using 50 mW ($P_s = 2.6 \times 10^6$) for the saturation power. Typical parameter values for a 1.55 μm index-guided InGaAsP laser of active volume $250 \times 2 \times 0.2 \mu\text{m}^3$ were used.

In particular, $\tau_p = 1.48$ ps, $\tau_e = 2.13$ ns, $R_{sp} = 2/\tau_p$, $G_N = 7.5 \times 10^3$ s⁻¹, and $N_0 = 10^8$. The oscillatory nature of $C(\tau)$ is due to relaxation oscillations. $C(\tau)$ tends to zero quickly at high powers because of a decrease in the damping time of relaxation oscillations.

The total intensity noise of the laser is quantified through the root-mean-square (RMS) noise level defined as $\sigma_p = \langle |\delta P|^2 \rangle^{1/2}$ and from eqn. 5 is related to $C(\tau)$ by the relation $\sigma_p = P\sqrt{[C(0)]}$. A quantity of practical interest is the signal-to-noise ratio (SNR) of the laser output defined as $SNR = P/\sigma_p = [C(0)]^{-1/2}$. By using $\tau = 0$ in eqn. 11, the SNR is found to be given by

$$SNR = \left(\frac{2\Gamma_R P}{R_{sp}} \right)^{1/2} \left(1 + \frac{\Gamma_e^2}{\Omega_R^2 + \Gamma_R^2} \right)^{-1/2} \quad (13)$$

Because Γ_R , Γ_e , and Ω_R depend on the laser power through eqns. 8 and 12, the SNR changes considerably with the power. Fig. 2 shows the variation of SNR with output power for three different values of the saturation power. Other parameters are identical to those of Fig. 1. The most notable feature of Fig. 2 is that the nonlinear gain leads to a saturation of the SNR for $p > 1$ such that the saturated value is smaller for lower values of P_s . This behaviour can be understood by noting that, except for very large values of p , the Γ_e term in eqn. 13 is

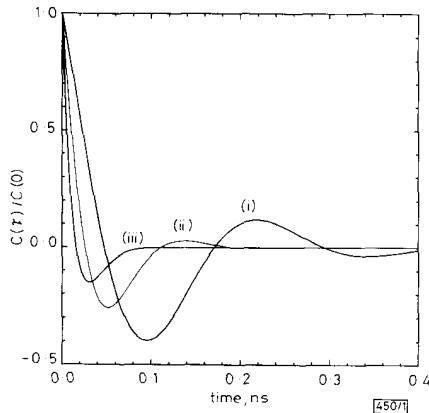


Fig. 1 Temporal variation of intensity autocorrelation function for various output powers

- (i) 3 mW
 - (ii) 10 mW
 - (iii) 50 mW
- Saturation power = 50 mW in all cases

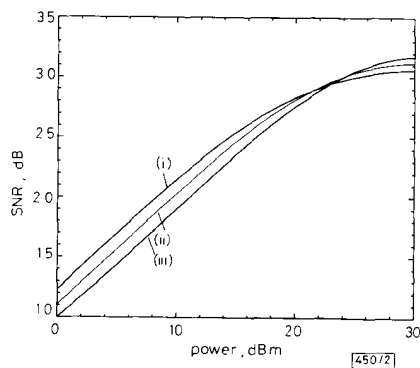


Fig. 2 Signal-to-noise ratio of laser output as function of output power for various saturation powers

- (i) 50 mW
- (ii) 100 mW
- (iii) 200 mW

negligible because, generally, $\Gamma_e \ll \Omega_R$. The SNR is then given by a remarkably simple expression.

$$SNR = (2\Gamma_R P/R_{sp})^{1/2} \quad (14)$$

Eqn. 14 clearly shows that spontaneous emission is the physical mechanism behind the laser noise. If the damping rate of relaxation oscillation were power independent, SNR would increase as \sqrt{P} with an increase in the output power. The power dependence of Γ_R can be incorporated by using eqns. 8–10. The SNR is then given by

$$SNR = \left[1 + \frac{P}{R_{sp}\tau_e} + \frac{G_N P^2}{R_{sp}} \left(1 + \frac{P}{P_s} \right)^{-1/2} + \frac{P^2}{2R_{sp}\tau_e P_s} \left(1 + \frac{P}{P_s} \right)^{-3/2} \right]^{1/2} \quad (15)$$

where $p = P/P_s$ was used and τ_e was assumed to be constant for simplicity. Eqn. 15 is the main result of this paper. It shows how the SNR changes with an increase in the laser power. Near or below threshold, $SNR = 1$, because the laser behaves as a thermal source. At a power level above a few milliwatts, the last term dominates. By using $R_{sp} = n_{sp}/\tau_p$, where n_{sp} is the spontaneous emission factor, and keeping only the last term in eqn. 15, we obtain

$$SNR = \left(\frac{P_s}{2n_{sp}} \right)^{1/2} \frac{P/P_s}{(1 + P/P_s)^{3/4}} \quad (16)$$

For $P \ll P_s$, SNR increases linearly with P as seen in Fig. 2. For $P > P_s$, SNR begins to saturate to a value determined by P_s . For typical parameter values $P_s \approx 4 \times 10^6$ and $n_{sp} = 2$, the limiting value of SNR is about 30 dB. Note that for $P \gg P_s$, eqn. 13 should be used in place of eqn. 16. The main conclusion is that the nonlinear gain provides a fundamental limit on the SNR of the laser output.

In summary, the nonlinear gain affects the intensity noise of semiconductor lasers significantly and must be considered for output powers above 10 mW. In its absence the SNR would keep improving with an increase in the laser power. However, its presence leads to a fundamental limit on SNR in the range of about 30 dB. The results of this Letter are important for a fundamental understanding of the intensity noise. At the same time, they may find applications in the design of subcarrier-multiplexed lightwave systems where intensity noise may be a limiting factor.

Acknowledgments: This work is supported by the US Army Research Office, the Joint Services Optics program, and the National Science Foundation.

G. P. AGRAWAL
The Institute of Optics
University of Rochester
Rochester, New York 14627, USA

24th October 1990

References

- 1 AGRAWAL, G. P., and DUTTA, N. K.: 'Long-wavelength semiconductor lasers' (Van Nostrand Reinhold Company, New York, 1986), Chap. 5
- 2 HENRY, C. H.: 'Phase noise in semiconductor lasers', *J. Lightwave Technol.*, 1986, **LT-4**, pp. 298–311
- 3 WELFORD, D., and MOORADIAN, A.: 'Output power and temperature dependence of the linewidth of single-frequency cw (GaAl)As diode lasers', *Appl. Phys. Lett.*, 1982, **40**, pp. 865–867
- 4 VAHALA, K., and YARIV, A.: 'Occupation fluctuation noise: A fundamental source of linewidth broadening in semiconductor lasers', *Appl. Phys. Lett.*, 1983, **43**, pp. 140–142
- 5 AGRAWAL, G. P., and ROY, R.: 'Effect of injection-current fluctuations on the spectral linewidth of semiconductor lasers', *Phys. Rev. A*, 1988, **37**, pp. 2495–2501
- 6 KIKUCHI, K.: 'Origin of residual semiconductor-laser linewidth in high-power limit', *Electron. Lett.*, 1988, **24**, pp. 1001–1002
- 7 KRÜGER, U., and PETERMANN, K.: 'The semiconductor laser linewidth due to the presence of side modes', *IEEE J. Quantum Electron.*, 1988, **24**, pp. 2355–2358

- 8 AGRAWAL, G. P.: 'Intensity dependence of the linewidth enhancement factor and its implications for semiconductor lasers', *IEEE Photonics Technol. Lett.*, 1989, 1, pp. 212-214
- 9 AGRAWAL, G. P.: 'Effect of gain and index nonlinearities on single-mode dynamics in semiconductor lasers', *IEEE J. Quantum Electron.*, November 1990, 26, pp. 1901-1909

BALANCED TUNED RECEIVER FRONT END WITH LOW NOISE AND HIGH COMMON MODE REJECTION RATIO

Indexing terms: Receivers, Optical receivers

A balanced optical receiver front-end suitable for Gbit/s heterodyne detection in coherent optical communication systems is presented. The transimpedance is 70 dB Ω with ± 2 dB ripple over the passband from 2 to 4.4 GHz. The ripple was reduced to ± 0.5 dB within a passband from 2.1 to 4.4 GHz by manual tuning of the circuit. The equivalent input noise spectral density is below 4 pA/ $\sqrt{\text{Hz}}$ and the common mode rejection ratio better than 26 dB. Standard commercial photodiodes and packaged components are used, and the circuit is implemented in conventional printed circuit board techniques.

Introduction: To use coherent heterodyne system configurations effectively and to take full advantage of the potential sensitivity improvement over direct detection systems it is essential to develop low-noise heterodyne receiver front ends. So far this has proven to be difficult especially for Gbit/s applications because of the parasitics of typical photodiodes. The best results that have been obtained with bandwidths of 2 GHz or more have used inductive tuning² and have obtained typical equivalent input noise spectral densities of around 10 pA/ $\sqrt{\text{Hz}}$ ^{2,3} for front-ends with one photodiode. In many systems the influence of relative intensity noise (RIN) on the local oscillator laser can be important.⁴ The requirements to the RIN level can be significantly eased using a balanced (two photodiode) receiver front end, but this in turn tends to increase the influence of photodiode parasitics and requires careful coupling of the photodiodes. Here, we present a design, suitable for Gbit/s applications, which simultaneously gives a high common mode rejection ratio due to the balancing and the lowest level of the noise spectral density reported so far.

Front-end design: The design is schematically shown in Fig. 1. We use two back-illuminated *pin* photodiodes each having

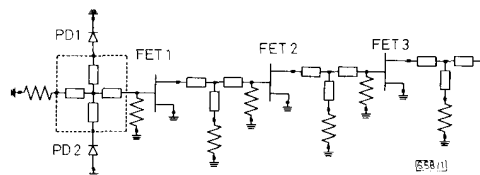


Fig. 1 Receiver front-end schematic diagram
Tuning network is contained by dotted box

parasitic capacitances of 0.2 pF, inductive parasitics from the bond wires of 4 nH and a serial parasitic resistance of 15 Ω including the parasitics of the ceramic chip carrier. We use commercial packaged microwave GaAs FET transistors for the three-stage amplifier. Transformer tuning¹ is used to compensate for the parasitics of the photodiode and the first amplifier stage. The transformer is implemented as a T-equivalent circuit consisting of 4 transmission lines in a completely symmetrical arrangement, indicated by the dotted rectangle in Fig. 1. This arrangement offers certain advantages over earlier designs based on either discrete inductors or on the parasitic inductance of bond wires.^{2,3} Firstly, a high degree of symmetry of the parasitic coupling between the

photodiodes and the tuning network is assured, which is a requirement to obtain a high common mode rejection ratio over the receiver frequency band. Secondly, a highly improved reproducibility is obtained by using conventional microstrip techniques. Thirdly, the arrangement makes the pigtail of the photodiodes easy because of the large physical separation of the two diodes of 9 mm.

Transmission line filters are used to obtain interstage matching between the three FET amplifier stages. The design has been done using the optimisation feature in the TOUCHSTONE microwave simulation program. The circuit is implemented on a 90 mm \times 32 mm Duroid substrate ($\epsilon_r = 2.33$). A complete receiver, consisting of the front-end circuit and a bias circuit for the transistors and the photodiodes is contained in a 90 mm \times 32 mm \times 10 mm milled aluminium box, which has a lowest cavity resonance frequency of 5 GHz. This is well above the passband of the electronics.

Results: In Fig. 2 we show the obtained transimpedance and the noise spectral density together with the theoretical predictions, in a frequency range from 1.2 to 5.2 GHz. There is a

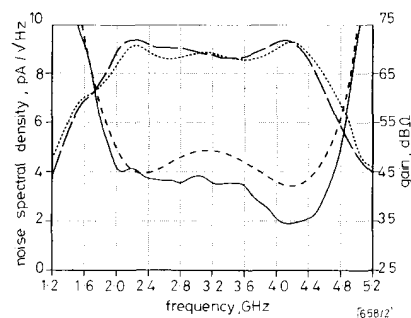


Fig. 2 Noise spectral density and transimpedance against frequency for front end

— noise (measured)
- - - noise (calculated)
- · - gain (measured)
· · · gain (calculated)

good agreement between the measurements and the theoretical curves, with a largest deviation of 2 dB on the gain and 1.6 pA/ $\sqrt{\text{Hz}}$ on the equivalent input noise spectral density. The transimpedance is flat within ± 2 dB over the passband from 2.0 to 4.4 GHz with a mean value of 70 dB Ω . The remaining passband ripple has been reduced to ± 0.5 dB in a band from 2.1 to 4.4 GHz by manual tuning of the circuit. See Fig. 3. An earlier version of the front end was used in a

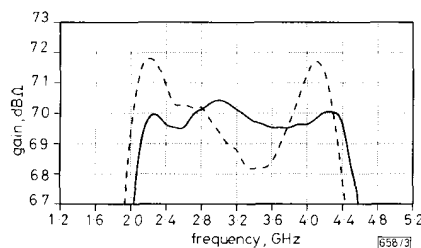


Fig. 3 Transimpedance for front end before and after tuning

- - - before tuning
— after tuning

636 Mbit/s SF-FSK system experiment with very good long term stability.⁵

The noise spectral density is below 4 pA/ $\sqrt{\text{Hz}}$ over the entire passband, with a lowest value of 1.9 pA/ $\sqrt{\text{Hz}}$ at 4.2 GHz. To our knowledge this density value is the lowest reported for a signal bandwidth as broad as 2.4 GHz. The level corresponds to the level of the shot noise for 45 μW local oscillator power. Therefore, for a local oscillator power level of around 250 μW , we expect to have a system sensitivity within 1 dB of the shot noise limit.¹ It is worth noting that as